

Electronic Supplementary Information

Carborane-Triggered Metastable Charge Transfer State Leading to Spontaneous Recovery of Mechanochromic Luminescence

Deshuang Tu, Pakkin Leong, Zhihong Li, Rongrong Hu, Chao Shi, Kenneth Yin
Zhang, Hong Yan,* and Qiang Zhao*

I. General methods

II. Synthesis

III. X-ray structure determination

IV. Quantum yields determination

V. Spectral data

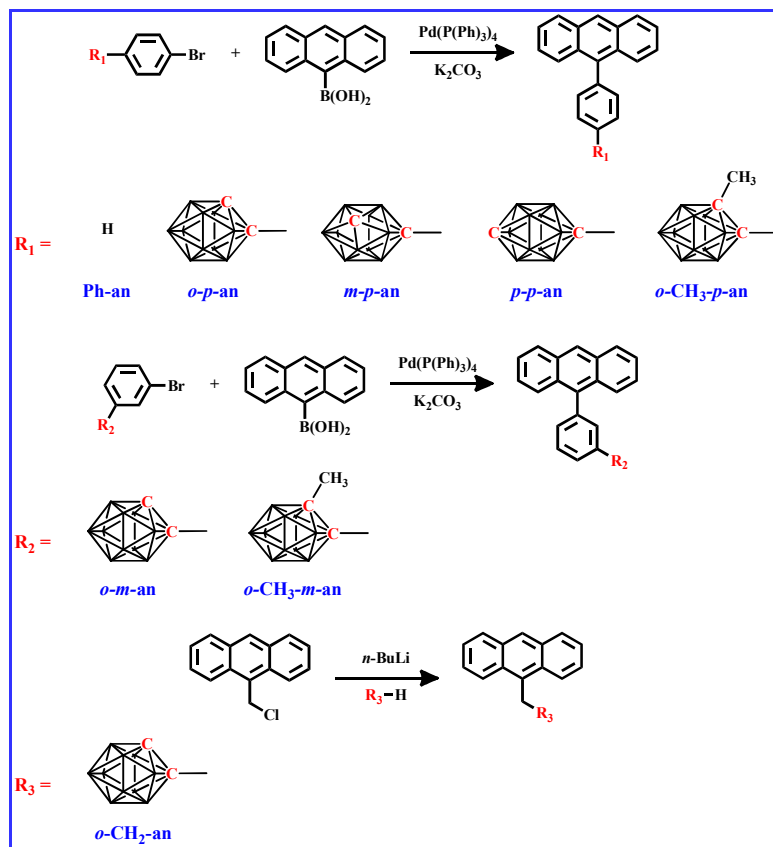
VI. Quantum chemical calculations

VII. References

I. General methods

All air- and moisture-sensitive reactions were carried out under an argon atmosphere. THF and Et₂O were dried over sodium and distilled under nitrogen. Dry DME and pyridine were obtained by refluxing and distilling over CaH₂ under nitrogen. *n*-BuLi (2.4 M in hexanes, Amethyst), 9-(chloromethyl) anthracene (Amethyst) were used as supplied. 1-(4-Bromophenyl)-*o*-carborane^{S1a}, 1-(3-bromophenyl)-*o*-carborane^{S1a}, (4-bromophenyl)-2-methyl-1,2-closo-carborane^{S1a}, (3-bromopeny)-2-methyl-1,2-closo-carborane^{S1a}, 1-(4-bromo-phenyl)-*m*-carborane, 1-(4-bromo-phenyl)-*p*-carborane^{S1b}, 1-(3-bromophenyl)-*p*-carborane^{S1b}, anthracen-9-ylboronic acid^{S1c}, Ph-an^{S1d} was synthesized according to literature procedures. The ¹H, ¹³C and ¹¹B NMR spectra were measured at room temperature by using Bruker DRX-500. CDCl₃ was used as deuterated reagent unless specified. Mass spectra measured with ESI-MS (LCQ Fleet, Thermo Fisher Scientific). Fluorescence spectral measurements were carried out by using a Hitachi F-4600 fluorescence spectrophotometer. Electronic absorption spectra were recorded with Shimadzu UV-2550 spectrophotometers. Elemental analyses for C and H were performed on a Vario MICRO elemental analyzer.

II. Synthesis



Scheme S1. The synthetic route for carborane-functionalized anthracene derivatives.

o-p-an: A mixture of 1-(4-bromophenyl)-*o*-carborane (150.0 mg, 0.50 mmol) and anthracene-9-ylboronic acid (133.2 mg, 0.60 mmol), Pd(PPh₃)₄ (23.0 mg, 0.02 mmol), K₂CO₃ (165.6 mg, 1.20 mmol) THF (20.0 mL) was refluxed for 24 h under argon. After cooling down to r.t., the

resulting mixture was extracted with CH_2Cl_2 (3×50.0 mL) and the combined organic layers were dried (MgSO_4). Removal of the solvents in vacuo gave a residue, which was subjected to column chromatography on silica gel. Elution with *n*-hexane to give white solid 81.0 mg, yield: 41 %. ^1H NMR (500 MHz, CDCl_3) δ 8.54 (s, 1H), 8.07 (d, $J = 8.4$ Hz, 2H), 7.71 (d, $J = 8.0$ Hz, 2H), 7.56 (d, $J = 8.7$ Hz, 2H), 7.49 (m, 2H), 7.43 (d, $J = 8.0$ Hz, 2H), 7.38 (m, 2H), 4.12 (s, 1H, carborane), 3.23–1.71 (br, 10H, B–H). ^{13}C NMR (126 MHz, CDCl_3) δ 140.91, 134.84, 132.70, 131.75, 131.28, 129.93, 128.51, 127.71, 127.27, 126.19, 125.79, 125.25, 76.49, 60.43. ^{11}B NMR (160 MHz, CDCl_3) δ 0.9 (3B), –5.9 (2B), –10.4 (3B), –11.5 (2B). IR(KBr): (ν cm^{-1}) 2571 (B–H). $\text{C}_{22}\text{H}_{24}\text{B}_{10}$ calcd: C, 66.64; H, 6.11. Found: C, 66.38; H, 6.34. EI-MS (*m/z*): 395.2 (M^+ , 100%).

m-p-an was also synthesized by the same procedure as ***o-p-an***. White solid. 118.0 mg, 60 %. ^1H NMR (500 MHz, CDCl_3) δ 8.50 (s, 1H), 8.04 (d, $J = 8.5$ Hz, 2H), 7.62 (t, $J = 8.5$ Hz, 2H), 7.61–7.56 (m, 2H), 7.46 (m, 2H), 7.36 (m, 2H), 7.33 (d, $J = 8.3$ Hz, 2H), 3.10 (s, 1H, carborane), 3.29–1.71 (br, 10H, B–H). ^{13}C NMR (126 MHz, CDCl_3) δ 139.32, 135.47, 134.33, 131.22, 131.15, 129.93, 128.31, 127.76, 126.85, 126.39, 125.48, 125.08, 78.2, 55.2. ^{11}B NMR (160 MHz,) δ –0.5 (1B), –4.1 (1B), –7.1 (4B), –10.1 (2B), –11.9 (2B). IR(KBr): (ν cm^{-1}) 2598 (B–H). $\text{C}_{22}\text{H}_{24}\text{B}_{10}$ calcd: C, 66.64; H, 6.11. Found: C, 66.30; H, 6.29. EI-MS (*m/z*): 395.2 (M^+ , 100%).

p-p-an was also synthesized by the same procedure as ***o-p-an***. White solid. 128.0 mg, 65 %. ^1H NMR (500 MHz, CDCl_3) δ 8.48 (s, 1H), 8.02 (d, $J = 8.4$ Hz, 2H), 7.54 (d, $J = 8.8$ Hz, 2H), 7.47–7.42 (m, 2H), 7.40 (d, $J = 8.2$ Hz, 2H), 7.34 (m, 2H), 7.24 (d, $J = 8.2$ Hz, 2H), 2.82 (s, 1H, carborane), 3.17–1.73 (br, 10H, B–H). ^{13}C NMR (126 MHz, CDCl_3) δ 138.87, 135.98, 135.62, 131.20, 130.83, 129.93, 128.25, 126.94, 126.73, 126.45, 125.39, 125.04, 86.28, 59.82. ^{11}B NMR (160 MHz, CDCl_3) δ –9.0 (5B), –11.7 (5B). IR(KBr): (ν cm^{-1}) 2604 (B–H). $\text{C}_{22}\text{H}_{24}\text{B}_{10}$ calcd: C, 66.64; H, 6.11. Found: C, 66.28; H, 6.33. EI-MS (*m/z*): 395.3(M^+ , 35.40%).

o-m-an was also synthesized by the same procedure as ***o-p-an***. White solid. 128.0 mg, 65.0 %. ^1H NMR (500 MHz, CDCl_3) δ 8.54 (s, 1H), 8.07 (d, $J = 8.4$ Hz, 2H), 7.68 (d, $J = 7.7$ Hz, 1H), 7.56 (t, $J = 7.7$ Hz, 1H), 7.52 (d, $J = 7.7$ Hz, 2H), 7.48 (m, 3H), 7.39 (m, 3H), 4.02 (s, 1H, carborane), 3.03–1.74 (br, 10H, B–H). ^{13}C NMR (126 MHz, CDCl_3) δ 139.60, 136.65, 134.83, 133.87, 132.71, 131.21, 129.96, 128.89, 128.49, 127.27, 126.69, 125.92, 125.88, 125.16, 76.19, 59.82. ^{11}B NMR (160 MHz, CDCl_3) δ 1.4 (2B), –0.9 (1B), –5.6 (3B), –7.6 (2B), –9.6 (2B). IR(KBr): (ν cm^{-1}) 2588(B–H). $\text{C}_{22}\text{H}_{24}\text{B}_{10}$ calcd: C, 66.64; H, 6.11. Found: C, 66.34; H, 6.25. EI-MS (*m/z*): 395.2 (M^+ , 73.18%).

o-CH₃-p-an was also synthesized by the same procedure as ***o-p-an***. White solid 98.5 mg, 50 %. ^1H NMR (500 MHz, CDCl_3) δ 8.53 (s, 1H), 8.06 (d, $J = 8.5$ Hz, 2H), 7.86 (d, $J = 8.4$ Hz, 2H), 7.54 (d, $J = 8.7$ Hz, 2H), 7.47 (m, 4H), 7.38 (m, 2H), 3.25–1.74 (br, 10H, B–H), 1.88 (s, 3H). ^{13}C NMR (126 MHz, CDCl_3) δ 141.48, 134.74, 131.72, 131.20, 131.04, 130.10, 129.80, 128.44, 127.22, 126.03, 125.74, 125.17, 81.98, 75.12, 23.47. ^{11}B NMR (160 MHz, CDCl_3) δ 0.3 (1B), –1.2 (1B), –6.9 (8B). IR(KBr): (ν cm^{-1}) 2584 (B–H). $\text{C}_{23}\text{H}_{27}\text{B}_{10}$ calcd: C, 67.12; H, 6.61. Found: C, 66.85; H, 6.47. EI-MS (*m/z*): 410.3 (M^+ , 100%).

o-CH₃-m-an was also synthesized by the same procedure as ***o-p-an***. White solid. 128.0 mg, 65.0 %. ^1H NMR (500 MHz, CDCl_3) δ 8.55 (s, 1H), 8.07 (d, $J = 8.5$ Hz, 2H), 7.83 (d, $J = 7.9$ Hz, 1H), 7.73 (s, 1H), 7.62 (t, $J = 7.8$ Hz, 1H), 7.55 (d, $J = 7.4$ Hz, 1H), 7.49 (dd, $J = 18.1, 8.6$ Hz, 4H), 7.37 (m, 2H), 3.16–1.74 (br, 10H, B–H), 1.83 (s, 3H). ^{13}C NMR (126 MHz, CDCl_3) δ 139.57, 134.87, 133.85, 133.67, 133.39, 132.16, 131.23, 130.24, 129.98, 128.93, 128.52, 127.27, 125.84, 125.14, 81.81, 77.5, 23.21. ^{11}B NMR (160 MHz, CDCl_3) δ 0.4 (1B), –1.1 (1B), –6.0 (4B), –6.8

(4B). IR(KBr): (ν cm⁻¹) 2576 (B–H). C₂₃H₂₇B₁₀ calcd: C, 67.12; H, 6.61. Found: C, 66.91; H, 6.35. EI-MS (*m/z*): 410.3 (M⁺, 100%).

***o*-CH₂-an:** A 1.6 M solution of *n*-BuLi in hexanes (0.70 mL, 1.12 mmol) was added dropwisely to a solution of *o*-carborane (144.0 mg, 1.00 mmol) in dry Et₂O (8.0 mL) at 0 °C. Following the addition, the reaction mixture was stirred at 0 °C for 30 min and then at room temperature for 30 min. This colorless solution was added dropwisely at 0 °C to a solution of 9-(chloromethyl) anthracene (200.0 mg, 0.90 mmol) in dry Et₂O (30.0 mL). The reaction mixture was stirred at room temperature for 15 h. Water (15.0 mL) was then added, and stirring was continued for 30 min. Ethyl acetate was added to the mixture until all of the precipitate had dissolved. The organic layer was separated, washed with water, dried over MgSO₄, and concentrated to solid. Chromatography with elution by hexanes gave ***o*-CH₂-an** as white solid. Yield: 102.0 mg, 34.0%. ¹H NMR (500 MHz, CDCl₃) δ 8.49 (s, 1H), 8.13 (d, *J* = 9.0 Hz, 2H), 8.05 (d, *J* = 8.3 Hz, 2H), 7.63 (m, 2H), 7.50 (m, 2H), 4.64 (s, 2H), 3.35 (s, 1H). ¹³C NMR (126 MHz, CDCl₃) δ 131.29, 130.81, 129.58, 128.96, 127.18, 126.75, 125.18, 123.38, 75.06, 58.34, 34.29. ¹¹B NMR (160 MHz, CDCl₃) δ 1.5 (1B), -2.1 (1B), -6.6 (1B), -7.2 (3B), -8.5 (2B), -9.73 (2B). IR(KBr): (ν cm⁻¹) 2588 (B–H). C₁₇H₂₂B₁₀ calcd: C, 61.05; H, 6.63. Found: C, 60.78; H, 6.75. EI-MS (*m/z*): 333.3 (M⁺, 79.76%).

IV. X-ray structure determination

The X-ray diffraction data were collected on a Bruker Smart CCD Apex DUO diffractometer with graphite monochromated Mo K α radiation (λ = 0.71073 Å) using the ω -2θ scan mode. The data were corrected for Lorenz and polarization effects. The structure was solved by direct methods and refined on *F*² by full-matrix least-squares methods using SHELXTL-2000. All calculations and molecular graphics were carried out on a computer using the SHELX-2000 program package, Mercury and Diamond. The powder XRD patterns were recorded at room temperature on a BRUKER D8 ADVANCE X-ray diffractometer. CCDC 1061897 (***o*-p-an**), 1061905 (***o*-CH₃-m-an**) and 1061906 (***o*-CH₃-p-an**) contain the supplementary crystallographic data for this paper. These data can be obtained free of charge from The Cambridge Crystallographic Data Centre via www.ccdc.cam.ac.uk/conts/retrieving.html (or from the Cambridge Crystallographic Data Centre, 12, Union Road, Cambridge CB21EZ, UK; fax: (+44) 1223-336-033; or deposit@ccdc.cam.ac.uk).

Table S1. Crystallographic data for ***o*-CH₃-p-an**, ***o*-CH₃-m-an** and ***o*-p-an**.

	<i>o</i>-CH₃-p-an	<i>o</i>-CH₃-m-an	<i>o</i>-p-an
Empirical formula	C ₂₃ H ₂₆ B ₁₀	C ₂₃ H ₂₆ B ₁₀	C ₂₂ H ₂₄ B ₁₀
Molecular weight	410.50	410.54	396.51
Crystal size (mm ³)	0.30 × 0.26 × 0.24	0.30 × 0.26 × 0.24	0.30 × 0.26 × 0.24
Temperature(K)	296(2)	296(2)	296(2)
Radiation	Mo-K α (0.7103Å)	Mo-K α (0.7103Å)	Mo-K α (0.7103Å)
Crystal system	Monoclinic	Monoclinic	Triclinic
Space group	<i>P</i> 2(1)/ <i>c</i>	<i>P</i> 2(1)/ <i>n</i>	<i>P</i> - <i>I</i>
a (Å)	15.683(3)	7.684(3)	9.520(2)
b (Å)	13.493(2)	23.434(7)	13.825(3)

c (Å)	11.675(2)	12.637(4)	17.646(4)
α (°)	90.00	90.00	88.713(4)
β (°)	108.429(3)	94.433(6)	88.594(4)
γ (°)	90.00	90.00	79.932(4)
V (Å ³)	2344.0(7)	2268.8(13)	2285.7(8)
Z	4	4	4
D_c (g cm ⁻³)	1.163	1.202	1.152
μ (mm ⁻¹) absorbt.coeff	0.059	0.061	0.058
F (000)	856	856	824
θ rang (deg)	1.37/27.51	1.74 /27.46	1.15 /25.00
Reflections collected	19838(R _{int} =0.1231)	15005 (R _{int} =0.0447)	16937 (R _{int} =0.0768)
Indep. reflns	5275	5171	7988
Refns obs. [$I > 2\sigma(I)$]	3598	3055	3213
Data/restr./paras	5275/0/339	5171/0/339	7988/0/529
Goodness-of-fit of χ^2	1.051	1.008	1.141
R_1 , wR_2 (all data)	0.1049/0.2334	0.0982/0.1442	0.2062/0.1603
R_1 , wR_2 [$I > 2\sigma(I)$]	0.0731/0.1933	0.0496/0.1188	0.0839 /0.1393
Larg.peak/hole(e.Å)	0.379/-0.386	0.175/-0.246	0.160/-0.530

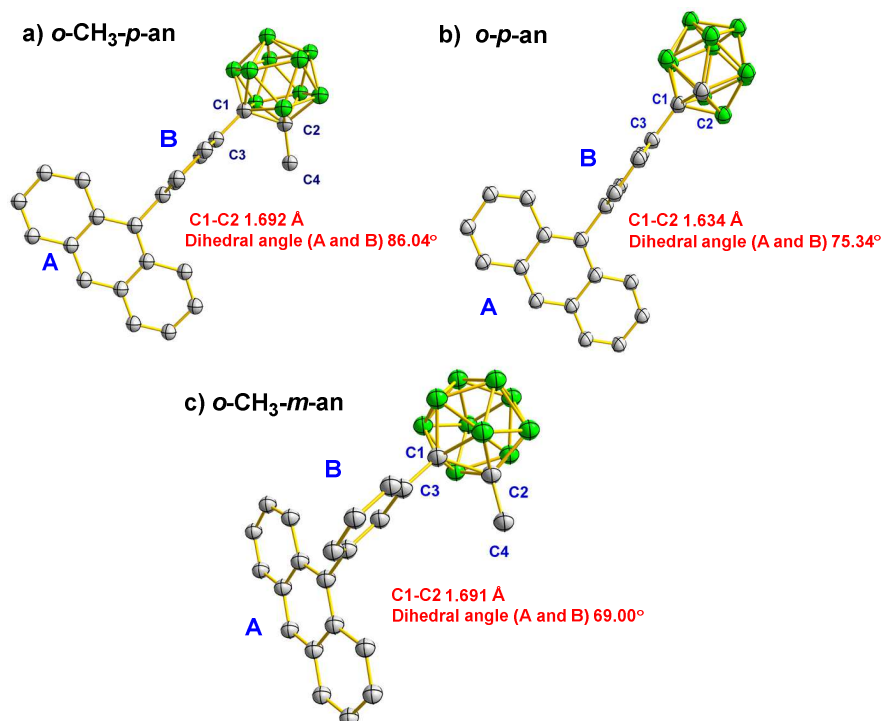
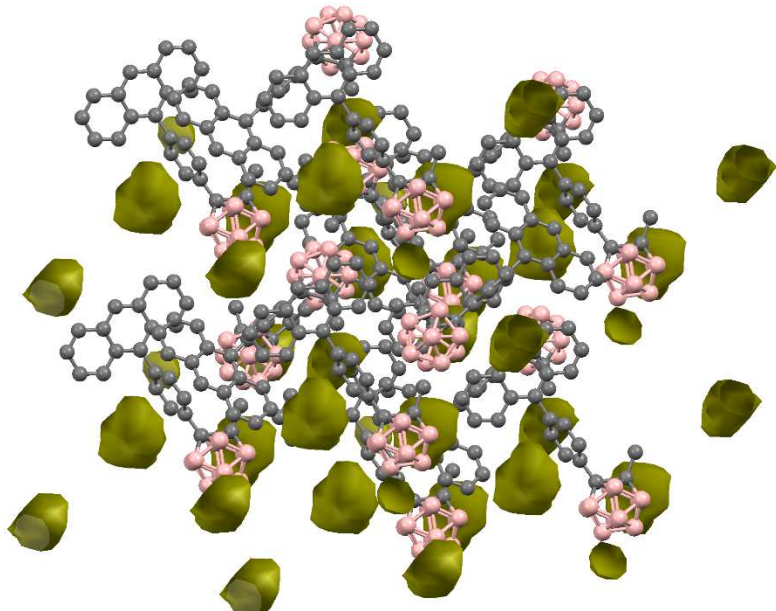


Fig. S1 The crystal structures for a) *o*-CH₃-*p*-an; b) *o*-*p*-an; c) *o*-CH₃-*m*-an.

a) C-H (*o*-carborane)... π (2.488 Å)



b) CH₂-H (*o*-carborane)...H-B and 2.400 (Å) CH₂-H...B (3.170 Å)

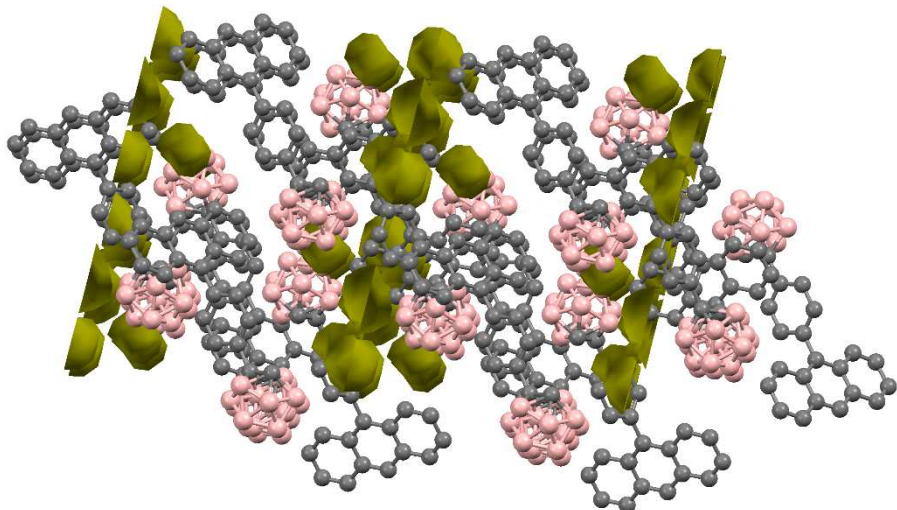


Fig. S2 The crystal packing structures for a) *o*-p-an; b) *o*-CH₃-p-an. The empty spaces occupy 3.2% and 2.1% unit cell volume for *o*-p-an and *o*-CH₃-p-an, respectively. The probe radius is 1 Å via the Mercury software.

IV. Quantum yields determination

Fluorescence spectroscopic studies were performed on a Hitachi F-4600 fluorescence spectrophotometer and Shimadzu UV-2550 spectrophotometers. The slit width was 5.0 nm for excitation and 5.0 nm for emission. Quinine sulfate in 0.5 M sulfuric acid ($\phi = 0.55$) was used as the standard for the fluorescence quantum yield calculation according to the absorption of the test sample. The spectroscopic grade solvents and a 1 cm quartz cuvette were used. Dilute solutions (10^{-6} M) were used to minimize the re-absorption effects. The quantum yields of Fluorescence were measured three times for each compound. Quantum yields were determined using the following equation:

$$Y_u = Y_s \times F_u/F_s \times A_s/A_u \times G_u^2/G_s^2$$

Y_s is the reported quantum yield of **quinine sulfate**. F_u is the area under the emission spectra of the measured compound. F_s is the area under the emission spectra of the standard. A_s is the absorbance at the excitation wavelength of the measured compound. A_u is the absorbance at the excitation wavelength of the standard. G_u is the refractive index of the solvent used. G_s is the refractive index of the solvent of the standard.

V. Spectra data

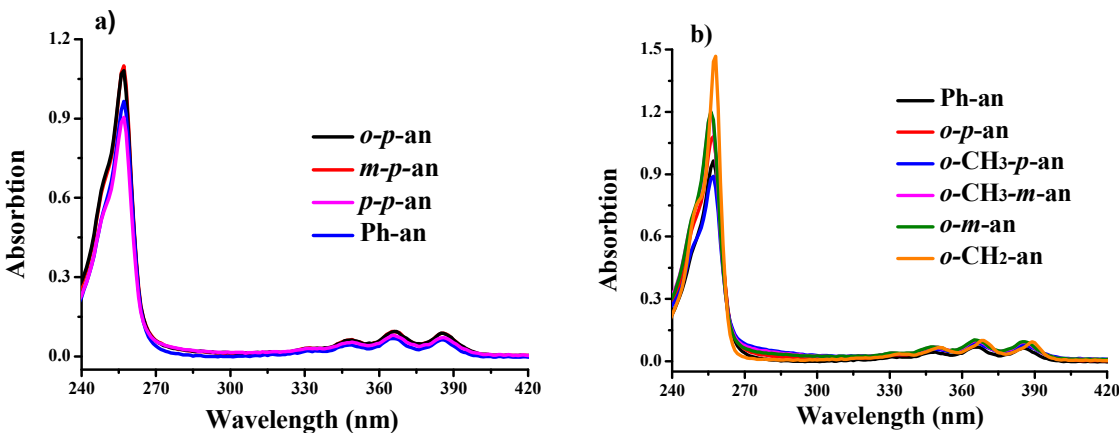


Fig. S3 The absorption spectra of a) **Ph-an**, ***o*-*p*-an**, ***m*-*p*-an**, ***p*-*p*-an**; b) **Ph-an**, ***o*-*m*-an**, ***o*- CH_3 -*p*-an**, ***o*- CH_3 -*m*-an**, ***o*-*p*-an**, ***o*- CH_2 -an** in CH_2Cl_2 (1.0×10^{-5} M) at room temperature.

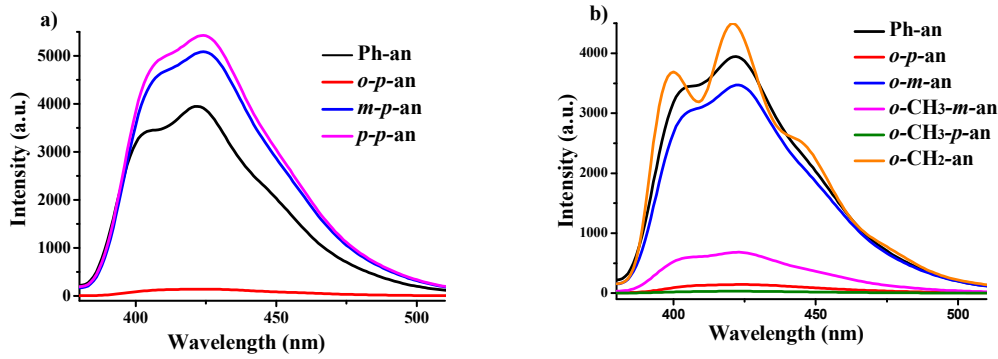
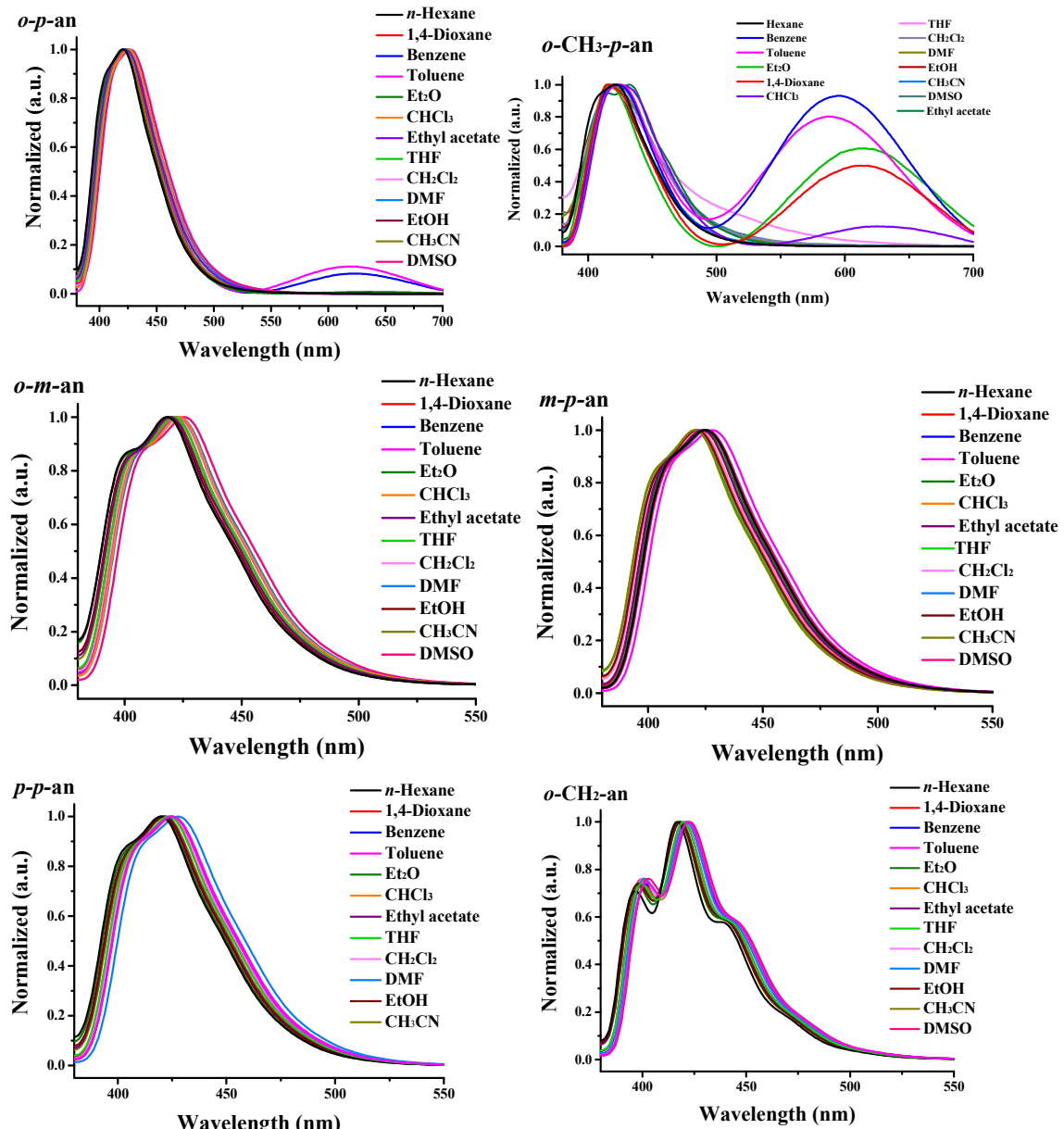


Fig. S4 The PL spectra of a) **Ph-an**, ***o*-*p*-an**, ***m*-*p*-an**, ***p*-*p*-an**; b) **Ph-an**, ***o*-*m*-an**, ***o*- CH_3 -*p*-an**, ***o*- CH_3 -*m*-an**, ***o*-*p*-an**, ***o*- CH_2 -an** in CH_2Cl_2 ($1.0 \times 10^{-6} \text{ M}$) at room temperature ($\lambda_{\text{ex}} = 366 \text{ nm}$).



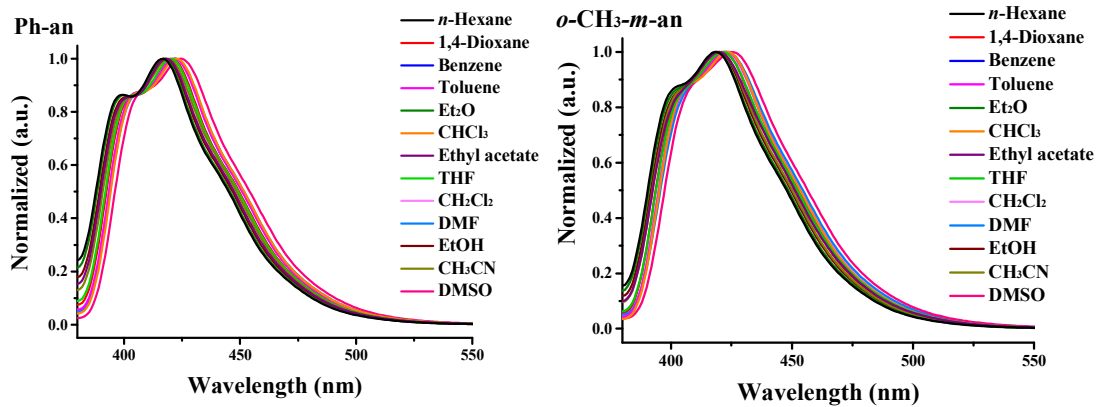


Fig. S5 Normalized PL spectra of *o*-*p*-an, *o*-CH₃-*p*-an, *o*-CH₃-*m*-an, *m*-*p*-an, *p*-*p*-an, *o*-*m*-an, *o*-CH₂-an and **Ph-an** in thirteen solvents with the same concentration (1.0×10^{-6} M) at room temperature ($\lambda_{\text{ex}} = 366$ nm).

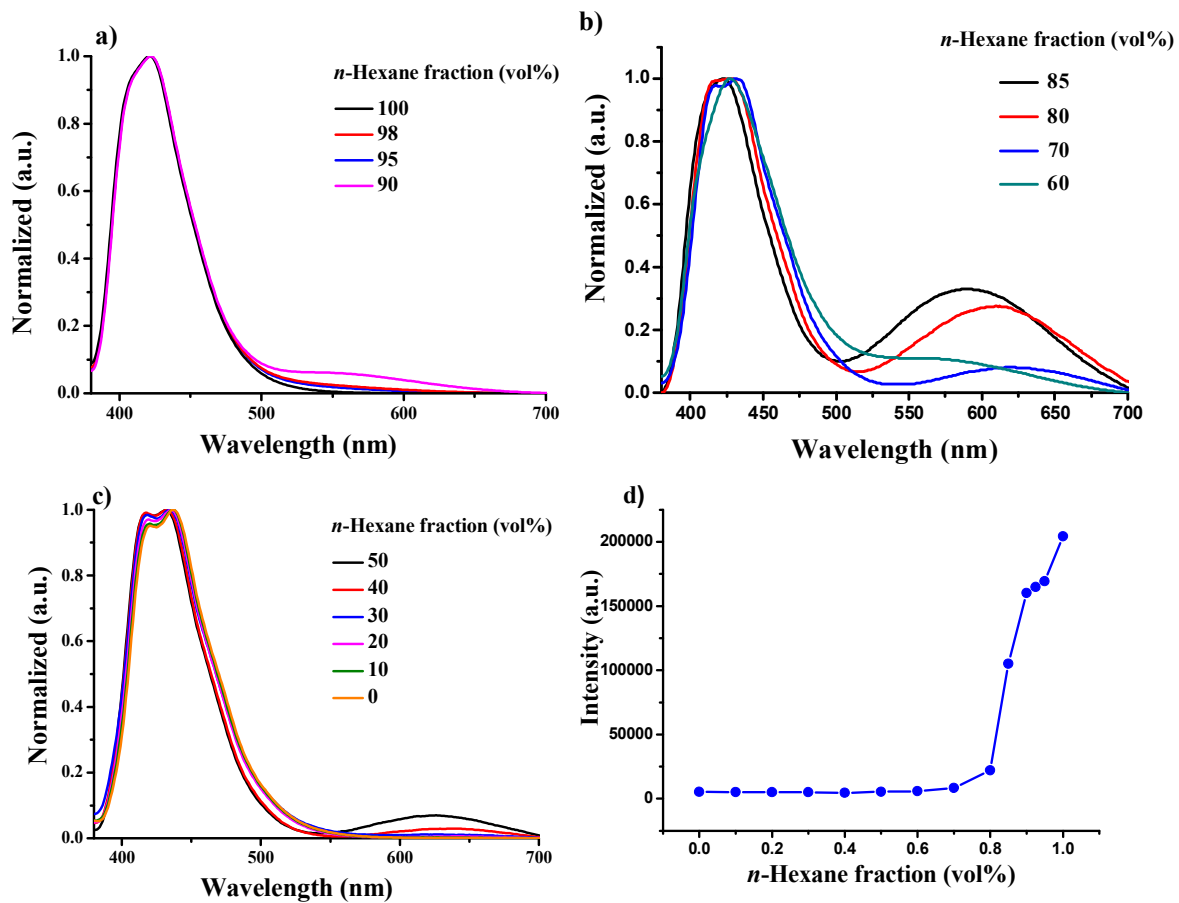


Fig. S6 a, b, c) The emission spectra of *o*-CH₃-*p*-an in the mixed solvents (CH₂Cl₂ and *n*-Hexane) with same concentration (2.0×10^{-6} M) at room temperature ($\lambda_{\text{ex}} = 366$ nm); d) Changes in the emission intensity with variations in *n*-Hexane fraction (vol%).

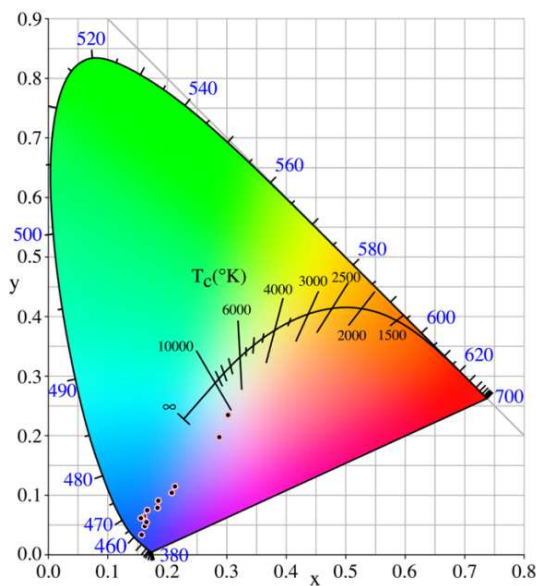
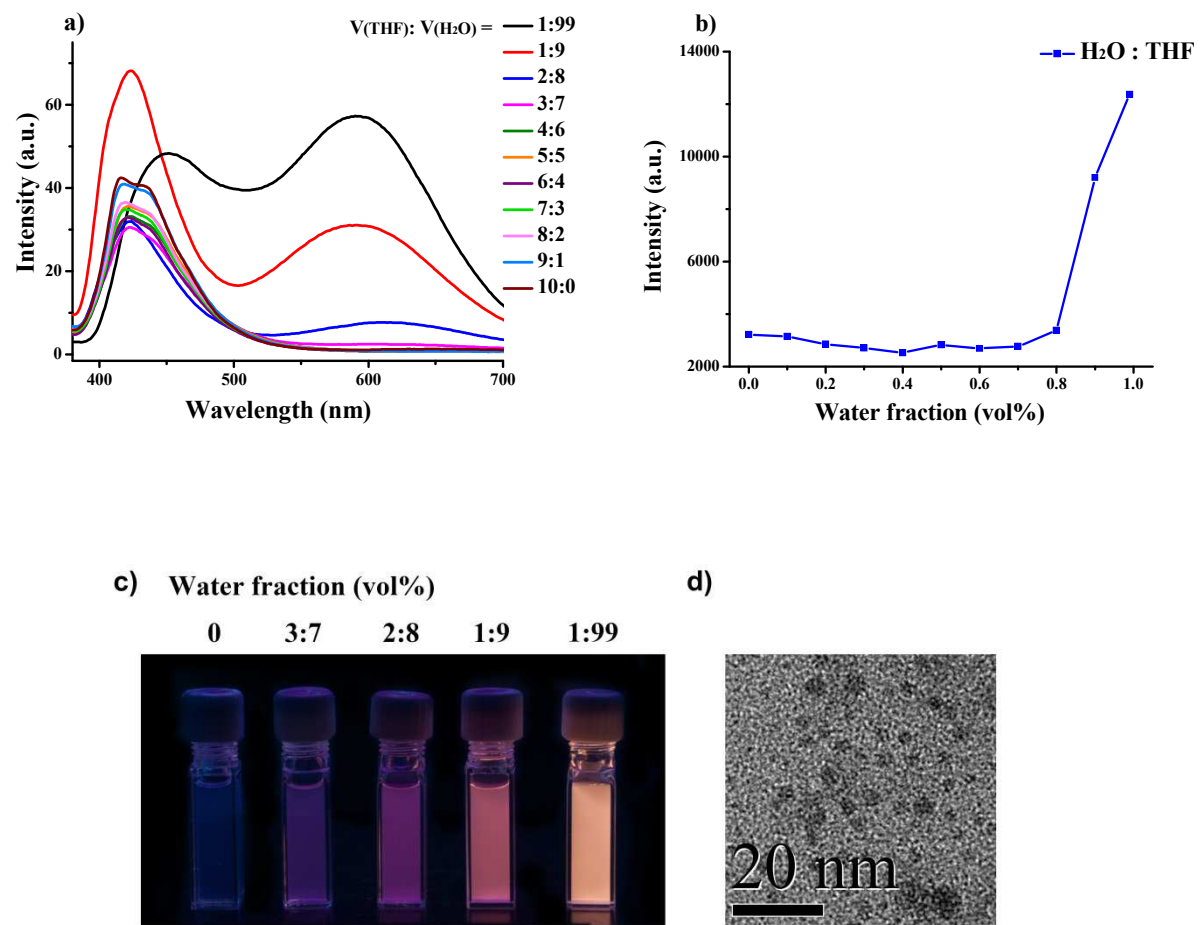


Fig. S7 Emission colors in a CIE 1931 chromaticity diagram of *o*-CH₃-*p*-an in different fractions of *n*-hexane.



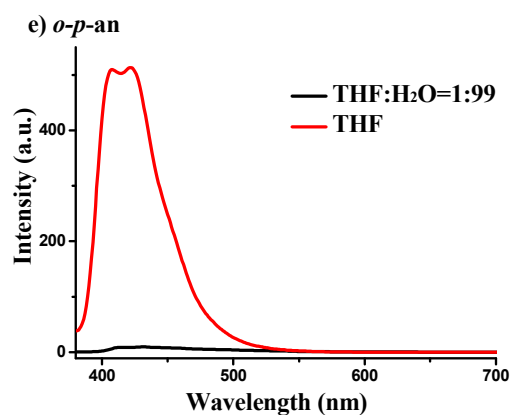
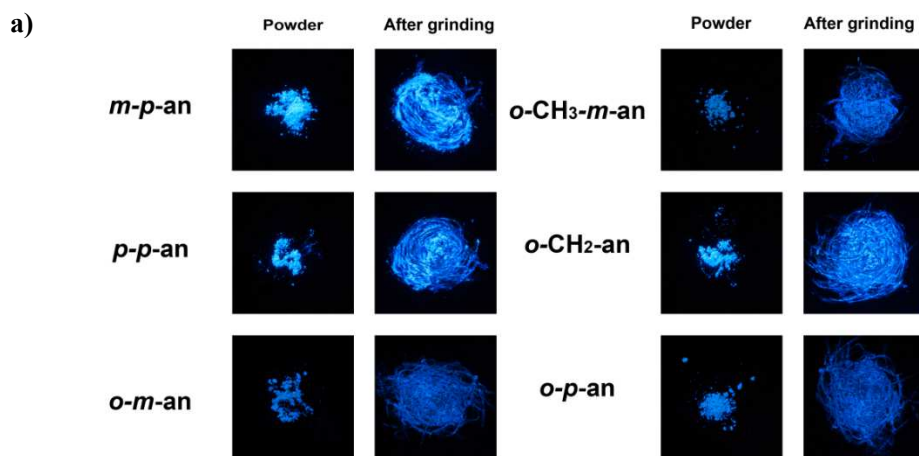


Fig. S8 a) PL spectra change in THF/H₂O with same concentration (2.0×10^{-6} M) at room temperature ($\lambda_{\text{ex}} = 366$ nm); b) Changes in the emission intensity with variations in water fraction; c) Photographs of *o*-CH₃-*p*-an in H₂O and THF mixtures with different fractions taken under UV illumination ($\lambda_{\text{ex}} = 365$ nm); d) TEM micrographs of *o*-CH₃-*p*-an obtained from THF/H₂O (1:99) solution; e) PL spectra of *o*-*p*-an in THF/H₂O = 1:99 and THF with concentration (5.0×10^{-6} M) at room temperature ($\lambda_{\text{ex}} = 366$ nm).



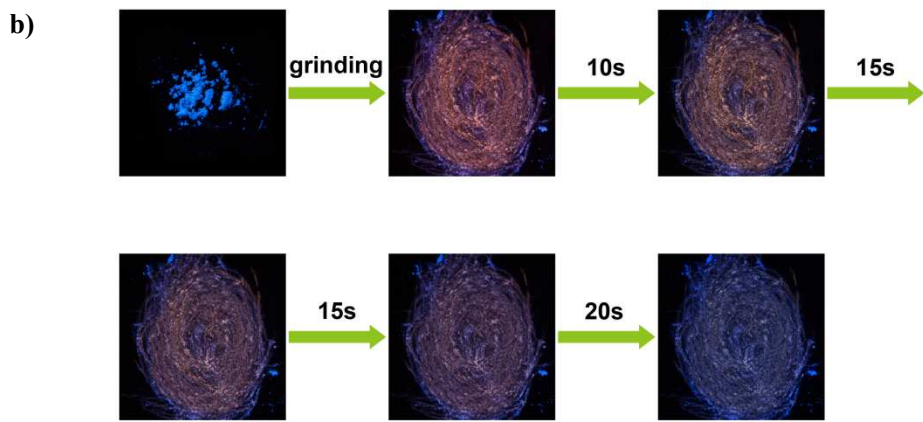


Fig. S9 a) Photographs of *o*-CH₃-*m*-an, *o*-*p*-an, *o*-*m*-an, *m*-*p*-an, *p*-*p*-an and *o*-CH₂-an before and after grinding under UV illumination; b) Dynamic photographs changes after grinding under UV illumination for *o*-CH₃-*p*-an ($\lambda_{\text{ex}} = 365 \text{ nm}$).

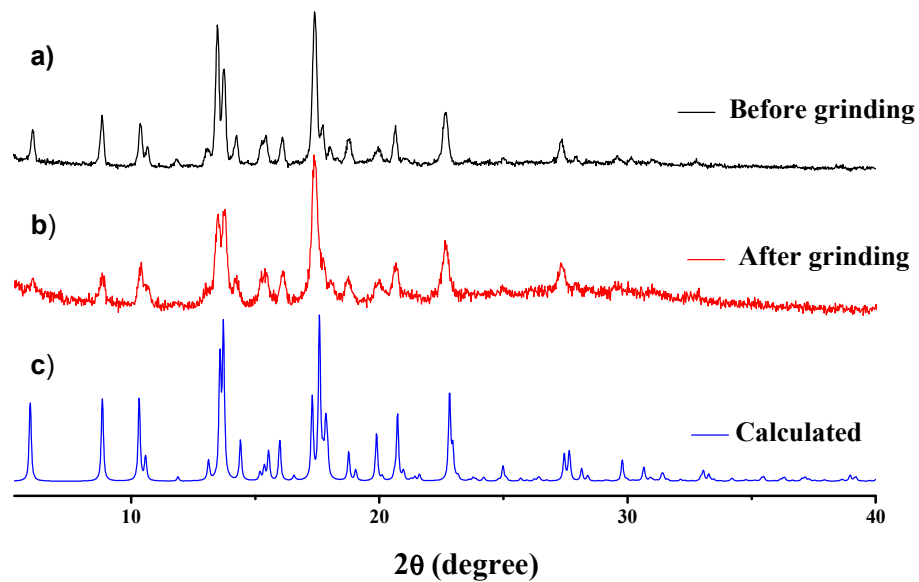


Fig. S10 XRD diffraction pattern of *o*-CH₃-*p*-an: a) before grinding; b) after grinding; c) calculated.

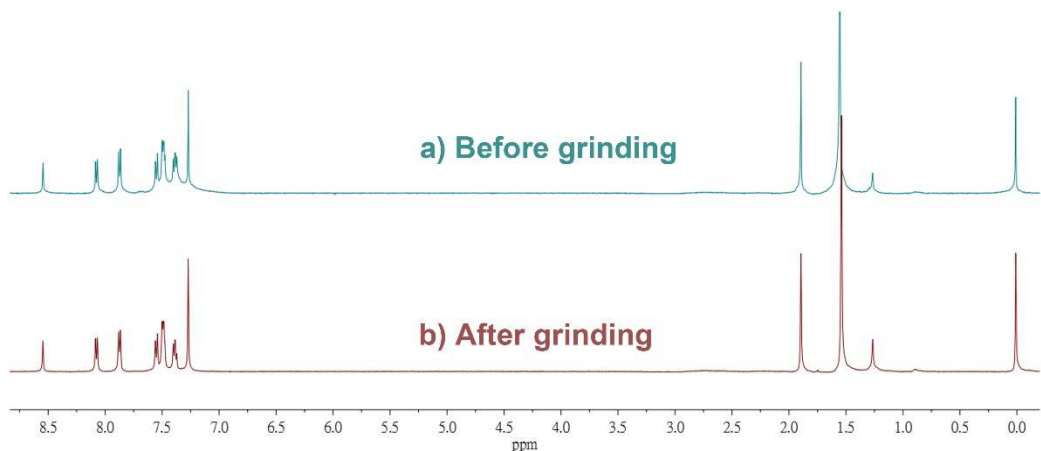
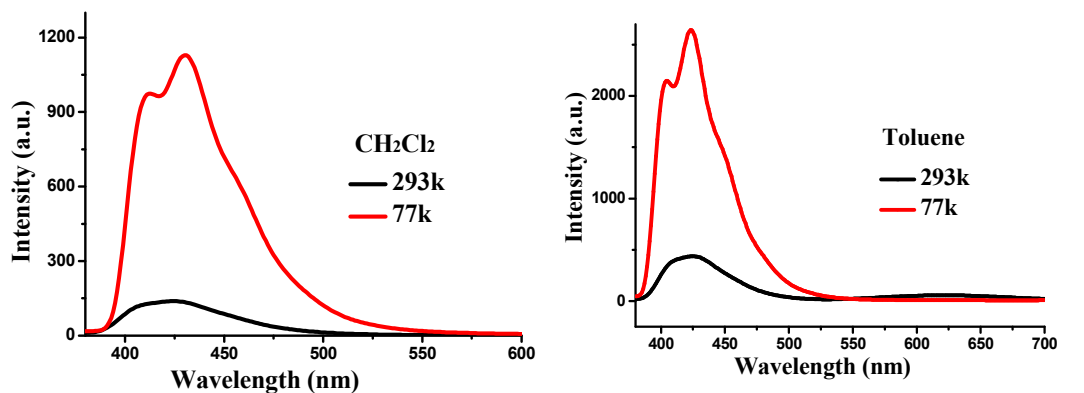
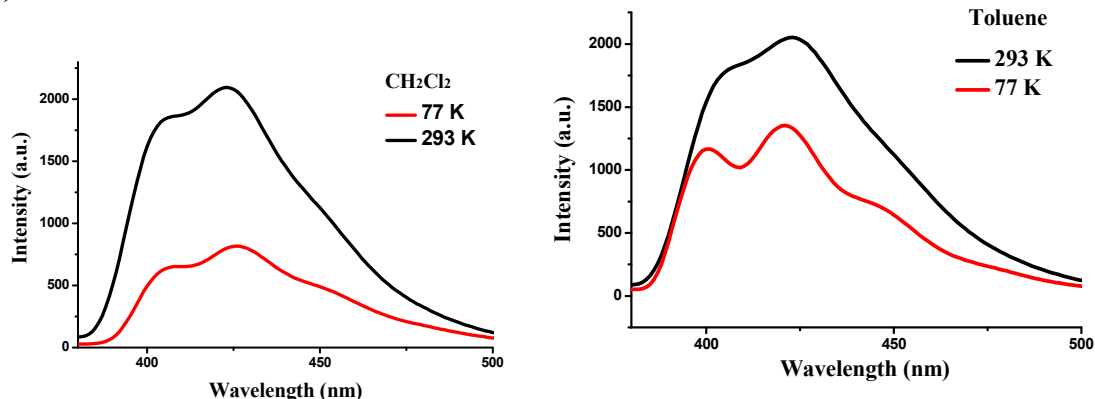


Fig. S11 ¹H NMR of *o*-CH₃-*p*-an in CDCl₃: (a) before grinding (b) after grinding.

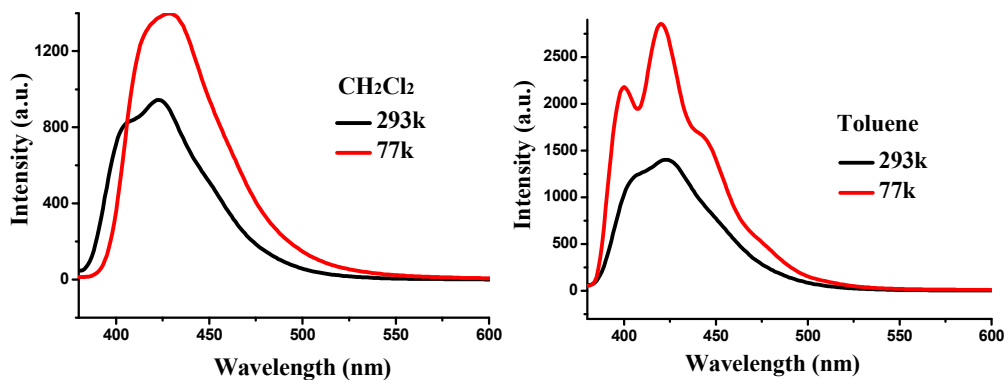
a) *o*-*p*-an



b) *o*-*m*-an



c) *o*-CH₃-*m*-an



d) *o*-CH₃-*p*-an

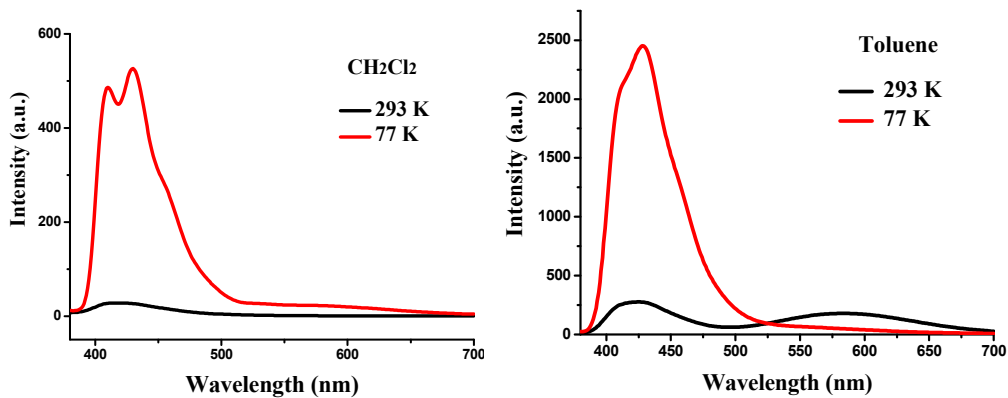


Fig. S12 PL spectra of a) *o*-*p*-an, b) *o*-*m*-an, c) *o*-CH₃-*m*-an, d) *o*-CH₃-*p*-an in CH₂Cl₂ and toluene with same concentration (2.0×10^{-6} M) at 77 K and 293 K ($\lambda_{\text{ex}} = 366$ nm).

VI. Quantum chemical calculations

The geometries of all compounds were optimized using the density functional theory (DFT) method. The electronic transition energies including electron correlation effects were computed by the time dependent density functional theory (TD-DFT) method using the B3LYP functional (TD-B3LYP). The 6-31G(d, p) basis set was used to treat all atoms. The different conformations for compound *o*-CH₃-*p*-an were generated from optimization ground state of geometries with a constrained dihedral angle. All calculations described here were performed by using the Gaussian 09 program^{S2}.

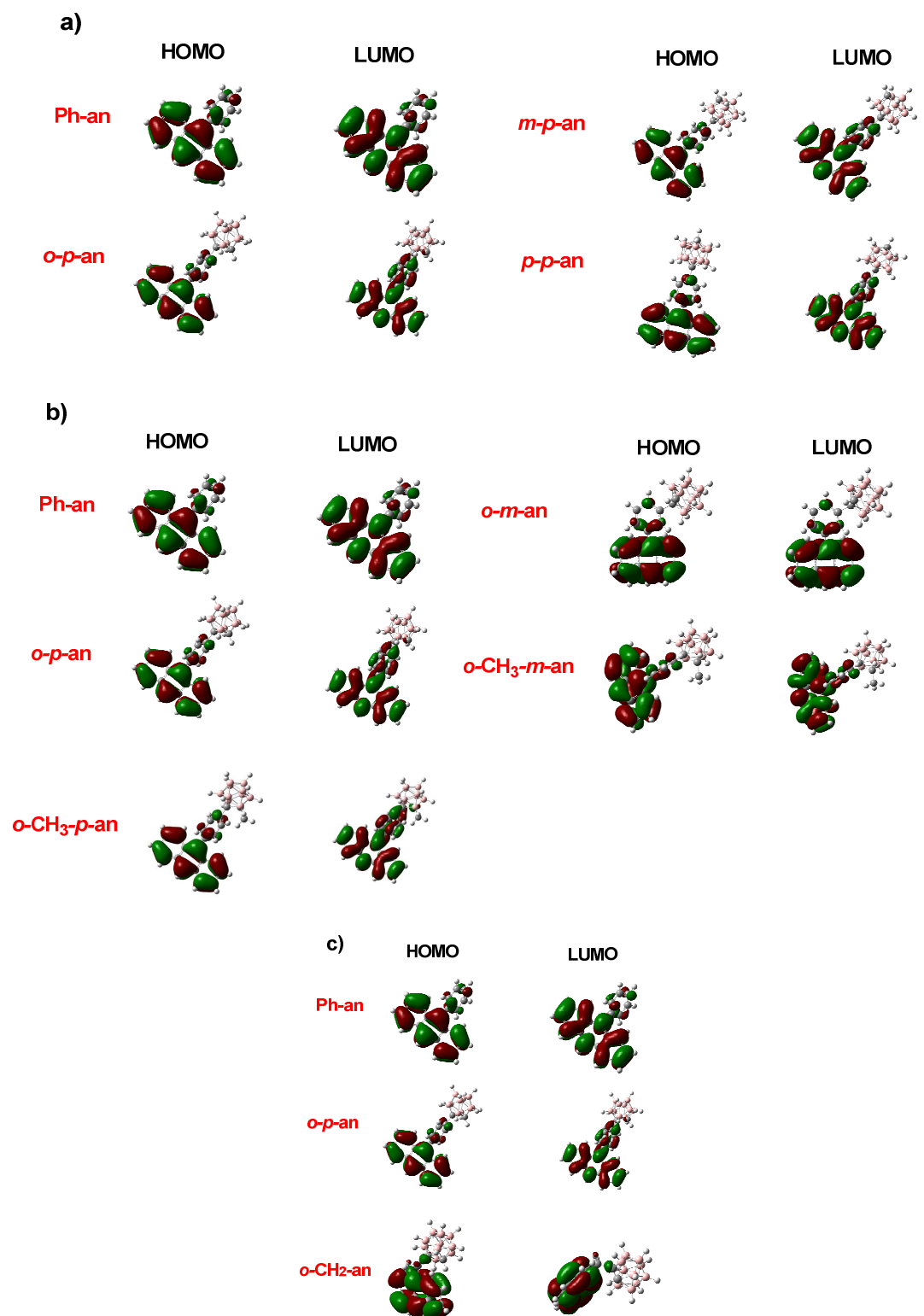


Fig. S13 Calculated HOMO and LUMO at the excited state by the TD-DFT method for a) Ph-an, *o*-*p*-an, *m*-*p*-an, *p*-*p*-an; b) Ph-an, *o*-*p*-an, *o*-CH₃-*m*-an, *o*-*m*-an; c) Ph-an, *o*-*p*-an, *o*-CH₂-an.

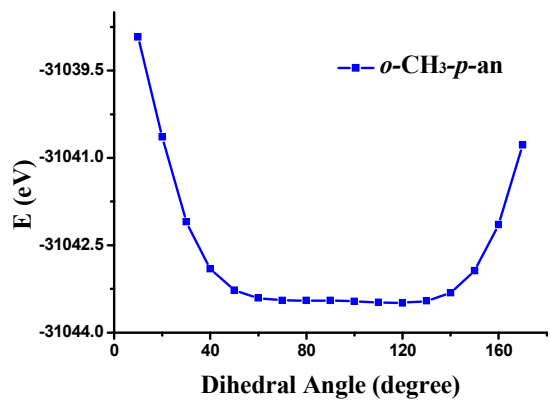


Fig. S14 The energy levels of *o*-CH₃-*p*-an with variable dihedral angle between anthracene and phenyl unit from 10° to 170°.

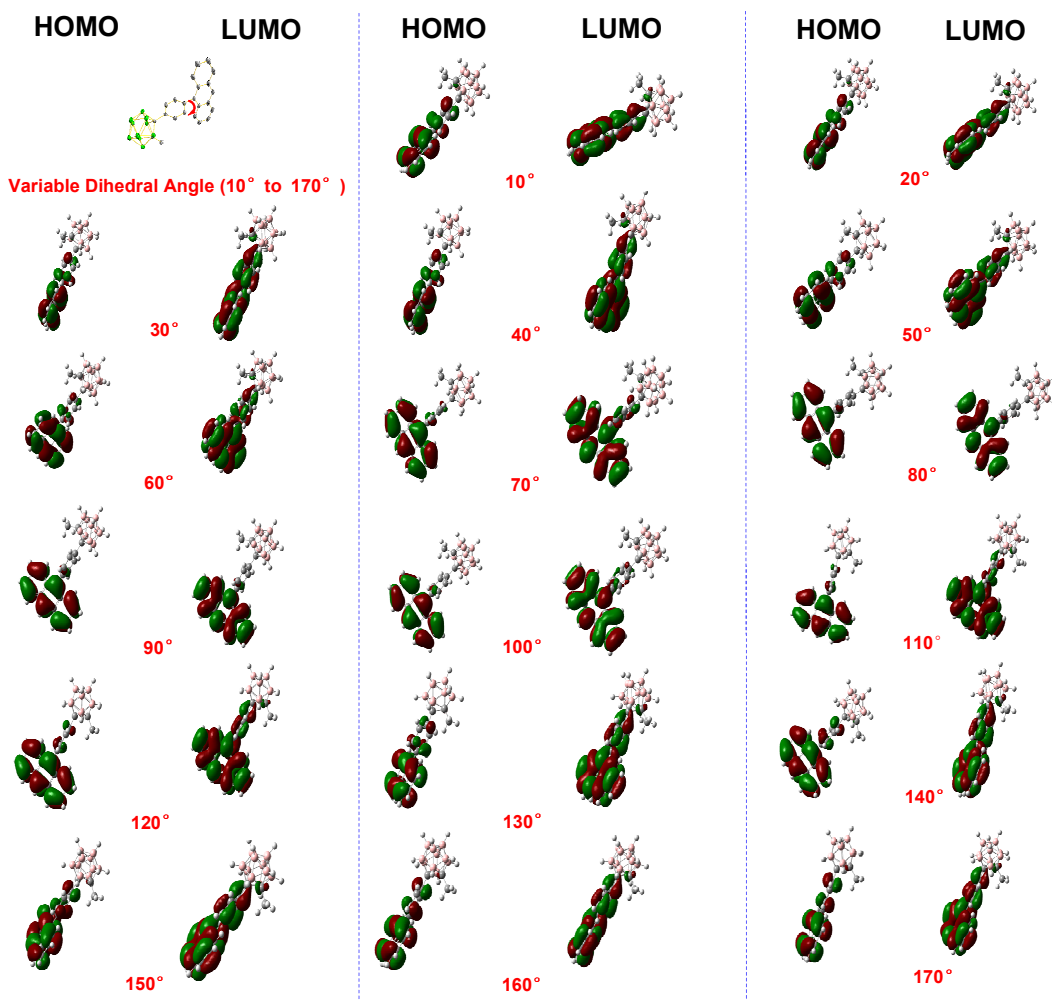


Fig. S15 Calculated HOMO and LUMO at the ground state for *o*-CH₃-*p*-an depending on dihedral angle from 10° to 170°.



Fig. S16 Photographs of *o*-CH₃-*p*-an after grinding one hour at 77 K and the temperature raised to r.t. ($\lambda_{\text{ex}} = 365$ nm).

VI. References

- S1 (a) T. Kim, H. Kim, K. M. Lee, Y. S. Lee, M. H. Lee, *Inorg. Chem.*, 2013, **52**, 160; (b) B. P. Dash, R. Satapathy, E. R. Gaillard, K. M. Norton, J. A. Maguire, N. Chug and N. S. Hosmane, *Inorg. Chem.*, 2011, **50**, 5485; (c) S. Kim, B. Yang, Y. Ma, J. Leecand, J. Park, *J. Mater. Chem.*, 2008, **18**, 3376; (d) J. Hu, Y. Pu, Y. Yamashita, F. Satoh, H. Sasabe, J. Kido, *J. Mater. Chem. C*, 2013, **1**, 3871.
- S2 M. J. Frisch, G. W. Trucks, H. B. Schlegel, G. E. Scuseria, M. A. Robb, J. R. Cheeseman, G. Scalmani, V. Barone, B. Mennucci, G. A. Petersson, H. Nakatsuji, M. Caricato, X. Li, H. P. Hratchian, A. F. Izmaylov, J. Bloino, G. Zheng, J. L. Sonnenberg, M. Hada, M. Ehara, K. Toyota, R. Fukuda, J. Hasegawa, M. Ishida, T. Nakajima, Y. Honda, O. Kitao, H. Nakai, T. Vreven, J. A. Montgomery Jr., J. E. Peralta, F. Ogliaro, M. Bearpark, J. J. Heyd, E. Brothers, K. N. Kudin, V. N. Staroverov, T. Keith, R. Kobayashi, J. Normand, K. Raghavachari, A. Rendell, J. C. Burant, S. S. Iyengar, J. Tomasi, M. Cossi, N. Rega, J. M. Millam, M. Klene, J. E. Knox, J. B. Cross, V. Bakken, C. Adamo, J. Jaramillo, R. Gomperts, R. E. Stratmann, O. Yazyev, A. J. Austin, R. Cammi, C. Pomelli, J. W. Ochterski, R. L. Martin, K. Morokuma, V. G. Zakrzewski, G. A. Voth, P. Salvador, J. J. Dannenberg, S. Dapprich, A. D. Daniels, O. Farkas, J. B. Foresman, J. V. Ortiz, J. Cioslowski, D. J. Fox, Gaussian 09, Revision B.01, Gaussian, Inc., Wallingford CT, 2010.